

## **Poly(vinyl alcohol)/modified cassava starch blends plasticized with glycerol and sorbitol**

Phetdaphat Boonsuk,<sup>1</sup> Apinya Sukolrat,<sup>2</sup> Sirinya Chantarak,<sup>1</sup> Antonios Kellarakis,<sup>3</sup> Chiraphon Chaibundit<sup>1,\*</sup>

<sup>1</sup> Division of Physical Science, Faculty of Science, Prince of Songkla University, Hat Yai, Songkhla, Thailand, 90110.

<sup>2</sup> Office of Scientific Instrument and Testing, Prince of Songkla University, Hat Yai, Songkhla, Thailand, 90110.

<sup>3</sup> UCLan Research Centre for Smart Materials, School of Natural Sciences, University of Central Lancashire, Preston PR1 2HE, UK.

\* Corresponding author: E-mail address: [chiraphon.c@psu.ac.th](mailto:chiraphon.c@psu.ac.th)

Telephone: +66 74 288364

**Abstract**

A series of blend films comprised 88% hydrolyzed poly(vinyl alcohol) (PVA) with native cassava starch (NCS), high-oxidized cassava starch (HCS), and pre-gelatinized cassava starch (PCS) was prepared via solution casting. The blends were plasticized with glycerol or glycerol-sorbitol mixture. The structure of each blend film was characterized by Fourier-transform infrared spectroscopy and X-ray diffraction analysis. Cross-sections of the PVA/HCS and PVA/PCS blend films, imaged by scanning electron microscopy, indicated a PVA-rich/starch-rich bilayer structure, irrespective of the type of plasticizer in the blend. High degree of swelling of the blend films resulted to the fast degradation. All blend films were completely degraded in soil after 4 days. Significantly, we identified a number of blend films showed greater strength and elongation at break than low density polyethylene, suggesting that these environmentally benign blends could be ideal candidates for widespread applications currently dominated by petroleum-derived products.

## 1. Introduction

Interest in biodegradable packaging has been increasing in response to the growing awareness of the environmental damage caused by accumulated petroleum-derived plastic waste.<sup>1-3</sup> In recent years, biodegradable natural polymers have been extensively researched<sup>4-6</sup> and, in certain applications, non-biodegradable synthetic polymers have been replaced by natural, or synthetic, biodegradable polymers.<sup>7</sup>

Poly(vinyl alcohol) (PVA), a biodegradable synthetic polymer, can be dissolved in hot water and used as a water-soluble film.<sup>8</sup> The degradation rate of PVA depended on the quantity of the residual acetate groups.<sup>9</sup> PVA is widely used in a range of industrial, commercial, medical and food applications and since the oral toxicity of PVA is very low, it is safe for use with food, medical, pharmaceutical and dietary supplement products.<sup>10</sup>

Starch, is an alternative biodegradable polymer from a renewable resource. It consists of amylose ( $\approx 25\%$ ), a linear polymer of  $\alpha$ -1,4-anhydro glucose units and amylopectin, a highly branched polymer of short  $\alpha$ -1,4-chains linked by  $\alpha$ -1,6-bonds, providing a crystalline structure.<sup>11</sup> Modification of starch via oxidation process can alter the physicochemical and thermal properties of oxidized-cassava starch such as water solubility in cold and hot water and rate of gelatinization. Oxidized starch can be prepared by the reaction between native starch and oxidizing agent under controlled temperature and pH.<sup>12-14</sup> The hydroxyl groups of native starch are oxidized to carbonyl and carboxyl groups,<sup>12,15</sup> which could be determined by the titrimetric method.<sup>15</sup> The reduction in hydroxyl groups in oxidized starch leads to the decrease in moisture content in the bioplastic films, low water absorption, and thus biodegradation delays.<sup>15</sup> It was reported that blending oxidized starch with PVA matrix reduced viscosity of the solution during the film formation due to the thixotropic nature of the starch.<sup>16</sup> The improvement of mechanical properties and physico-mechanical properties of oxidized starch-based bioplastic film was also reported. Introducing plasticizer such as

glycerol (Gly) or sorbitol (Sor) to the oxidized starch-based films could enhance water resistance and flexibility. The films showed low water vapor permeability and low solubility in water.<sup>17</sup> In addition, thermal stability of the plasticized oxidized starch-based films improved due to enhanced hydrogen bonding between polymers and plasticizer.<sup>18</sup>

Pre-gelatinization of starch either by cooking and drying processes leads to the complete structural disintegration of starch granules.<sup>19</sup> The molecular order in the starch granules is destroyed, and thus the solubility and the swelling capacity of the starch increase.<sup>20</sup> Using pre-gelatinized starch together with plasticizer was reported with high tensile strength but low strain and elongation at break. Enhancement in tensile strength of the films prepared from pre-gelatinized starch was due to an increase in material miscibility.<sup>21</sup>

Polymer blends of PVA/starch have poor mechanical properties,<sup>22-23</sup> that can be improved upon the addition of plasticizers such Gly<sup>2,3,6,24-27</sup> and Sor.<sup>28</sup> The physical and mechanical properties and water absorption of starch-based films can be adjusted using the binary mixture of plasticizers by varying type and content of each plasticizer. Moreover, the mixture of xylitol (Xy) with Sor was reported for easy handling, non-sticky, and low water absorption compared with Gly-Xy and Gly-Sor mixture.<sup>29</sup> Tensile strength and Young's modulus of the films decreases and the elongation at break increases with increasing the amount of plasticizers. In our previous work, four types of starch: native cassava starch (NCS), high-oxidized cassava starch (HCS), low-oxidized cassava starch (LCS) and pre-gelatinized cassava starch (PCS) were blended with 99% hydrolyzed PVA at the PVA to starch weight ratio of 7:3 and plasticized with Gly.<sup>6</sup> PVA endowed the blend films with high tensile strength, high degree of crystallinity, and strong resistance to biodegradation. Investigation of the miscibility of PVA and starch by SEM revealed that a bilayer structure was formed for the systems containing HCS, LCS and PCS.

In this work, we focused on three types of starch, namely NCS, HCS, and PCS that were blended with PVA (88% hydrolyzed) (starch to PVA weight ratio 1:1) in the presence of the plasticizer Gly and Gly-Sor mixture. The structure, mechanical properties, thermal behavior, and biodegradability of the blend films were systematically explored. Within this family of biodegradable materials, we identified compositions that exhibited fast biodegradation profiles combined with advanced mechanical properties, thus carrying promise as viable alternatives of petroleum-derived polyolefins in demanding applications.

## **2. Experimental**

### ***2.1 Materials***

Native cassava starch (NCS), food grade high-oxidized cassava starch (HCS), and pre-gelatinized cassava starch (PCS) were obtained from the Siam Modified Starch, Ltd., Thailand. Poly(vinyl alcohol) (88% hydrolyzed, MW 90,000-110,000, and viscosity 30.1 mPa·s) was from the Nippon Synthetic Chemical Industry Co., LTD. Glycerol (Gly) was from Sigma-Aldrich, Steinheim, Germany. Sorbitol (Sor) was from Ajax Finechem, NSW, Australia. All chemicals were used as received.

### ***2.2 Preparation of the blend films***

The PVA/starch blend films plasticized with Gly and Gly-Sor were prepared by the solution casting method. All blends containing different type of starch were prepared following this model. Briefly, 5 g of PVA were dissolved in 100 mL of water at 95 °C. Separately, 5 g of starch were dissolved in 100 mL of water at 95 °C. When the starch was dissolved, 3 g of Gly or the mixture of 1.5 g of Gly and 1.5 g of Sor were added and the mixture was stirred for 30 min using a kitchen mixer (Electrolux, EHM2000, speed no. 1). The PVA solution was then added to the starch/plasticizer solution. The mixture solution was

stirred for 30 min at 95 °C. The total volume was maintained by adding water. The solution was filtered through a kitchen sieve onto a polystyrene (PS) tray (20 cm × 29 cm) and left overnight at room temperature ( $T = 29 \pm 1$  °C) and dried the following day in an oven at 60 °C for 24 h. For comparison, PVA (10 g) films without starch were prepared using a similar method. All samples were named with type of starch and Gly for Gly plasticizer or Gly-Sor for mixed plasticizer.

### **2.3 Characterization**

Fourier-transform infrared spectroscopy (FTIR, Bruker Tensor 27) was used to record the FTIR spectra of the films in the frequency range of 600 to 4000  $\text{cm}^{-1}$  in attenuated total reflectance (ATR) mode with a diamond crystal. The samples were kept in a desiccator prior to testing. Both sides of the films were scanned.

Mechanical properties of the specimens were determined according to ASTM standard D638-03, Type V. The samples were prepared with the width = 3.18 mm, the distance between grip = 25 mm, and the film thickness =  $0.20 \pm 0.02$  mm). Determination of tensile strength and elongation at break of the samples was carried out with a Universal Testing Machine (Instron 3365) equipped with a 100 N load cell and operated at a cross-head speed of 20  $\text{mm min}^{-1}$  at 25 °C. Prior to testing, the samples were equilibrated for 7 days at 75% relative humidity (RH). Ten specimens were tested per formulation.

The morphology of blend films was investigated using scanning electron microscopy (SEM, Quanta 400). For cross-sectional morphology, cryo-fractured surfaces were prepared by immersing the films in liquid nitrogen before fracturing. For morphology after tensile testing, the samples were placed vertically on stubs. All specimens were coated with a thin layer of gold before observation.

X-ray diffraction of both sides of films were analyzed using a Phillips diffractometer (XRD, X'Pert MDI) operating at 40 kV and 30 mA. A scanning rate was  $3^\circ \text{ min}^{-1}$  with  $\text{CuK}\alpha$  radiation ( $\lambda = 1.5410 \text{ \AA}$ ). The scanning range of  $2\theta$  was from  $5^\circ$  to  $90^\circ$ . All samples were characterized within 1.5 months of their preparation.

Thermal properties of the films were characterized with differential scanning calorimetry (DSC, NETZSCH DSC 200F3). The sample, in an aluminum pan, was initially cooled to  $0^\circ \text{C}$ , then heated to  $250^\circ \text{C}$ , cooled from  $250^\circ \text{C}$  to  $0^\circ \text{C}$ , and finally heated again from  $0^\circ \text{C}$  to  $250^\circ \text{C}$  in a nitrogen atmosphere. The cooling and heating rates were controlled at  $10^\circ \text{C}/\text{min}$ . The degree of crystallinity ( $X_c$ ) of the films was calculated using Eq. 1:<sup>30</sup>

$$X_c (\%) = \frac{\Delta H_f}{(1 - \omega) \times \Delta H_f^0} \times 100 \quad (1)$$

where  $\Delta H_f$  was the apparent enthalpy of fusion of the films,  $\omega$  was the weight fraction of PVA in the blend, and  $\Delta H_f^0$  was the enthalpy of fusion of 100% crystalline PVA ( $141.932 \text{ J g}^{-1}$ ).<sup>31</sup>

The method of swelling testing was reported in Boonsuk et al.<sup>6</sup> Briefly, the samples ( $1.5 \text{ cm} \times 1.5 \text{ cm}$ ) were dried in an oven at  $60^\circ \text{C}$  for 24 h then immersed in water for 24 h. When the samples were removed from the vials, excess water on the surface of the swollen films was removed with filter paper. Six samples were determined per formulation. The degree of swelling (DS) was determined from Eq. (2):

$$\text{DS} (\%) = \frac{(w_e - w_0)}{w_0} \times 100 \quad (2)$$

where  $w_e$  was the weight of the sample at the absorbing equilibrium and  $w_0$  was the dry weight of the sample.

A soil burial test was carried out indoor using a method reported in Boonsuk et al.<sup>6</sup> In brief, the samples (1.5 cm × 1.5 cm) were dried in an oven at 60 °C for 24 h and then buried in soil at a depth of 5 cm of 500 mL cups. The soil was watered with 10 mL every other day. Six specimens were tested per formulation. The samples were observed after 1 day to 4 days in soil. The weight losses of the degraded samples were calculated using the following Eq. (3):

$$\text{weight loss (\%)} = \frac{(w_0 - w_d)}{w_0} \times 100 \quad (3)$$

where  $w_0$  and  $w_d$  were the weights of the dried sample before and after soil burial, respectively.

### 3. Results and discussion

#### 3.1 Structure

The FTIR spectra of top (T) and bottom (B) sides of the PVA/starch/Gly and PVA/starch/Gly-Sor blend films of all starch types are shown in Figure 1. The top side was exposed to the air while drying and the bottom side was in contact with the PS preparation tray. The peak assignments are listed in Table S1 and S2 in the Supporting Information. For comparison, the spectra of PVA, PVA/Gly, and PVA/Gly-Sor films are shown in Figure S1 in the supporting Information. All blend films show the peak position at  $\approx 3282\text{-}3283\text{ cm}^{-1}$ , which was attributed to the  $\text{-OH}$  stretching vibration of PVA, starch, Gly, and Sor.<sup>24,26</sup> This peak was shifted from  $\approx 3272\text{ cm}^{-1}$  as appeared in the spectra of PVA/Gly and PVA/Gly-Sor



films (Figure S1) indicating more interaction between –OH groups of starch and plasticizers than those of PVA and plasticizers. The peak intensity derived from the –OH stretching vibration of the oxidized starch was lower than that of the native starch because the hydroxyl groups were replaced by carbonyl and carboxyl groups during the oxidation.<sup>17</sup> The absorption bands at  $\approx 2939\text{ cm}^{-1}$  and  $\approx 2925\text{ cm}^{-1}$  were attributed to the –CH<sub>2</sub> stretching vibration.<sup>24,26,32</sup> The absorption bands at  $\approx 1730\text{ cm}^{-1}$  and  $\approx 1714\text{ cm}^{-1}$  were attributed to the C=O stretching vibration characteristic of residual acetate groups in the PVA.<sup>24</sup> These bands were more intense at the top side than the bottom side. The absorption bands at  $\approx 1650\text{ cm}^{-1}$  were attributed to the –OH bending of bound water.<sup>26,32</sup> The bottom side of all films showed the C–O stretching of the C–O–C groups in the  $\alpha$ -1,6-D- glycosidic linkage of starch at  $\approx 993\text{ cm}^{-1}$ <sup>1,32,33</sup> and the bending vibration of C–O–C groups in the  $\alpha$ -1,4-D- glycosidic linkage of the anhydrous glucose ring of starch at  $\approx 757\text{ cm}^{-1}$ .<sup>32</sup> These peaks were not present in the spectra of the top side, indicating a very low content of the starch component.

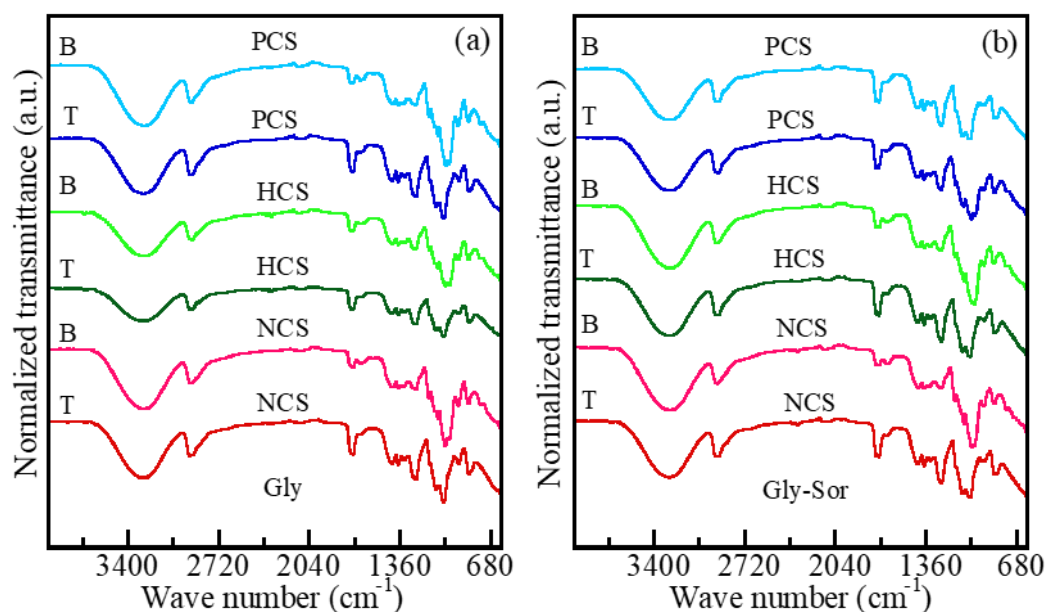


**Figure 1.** FTIR spectra of (a) PVA/starch/Gly and (b) PVA/starch/Gly-Sor films. Types of starch are indicated. T and B refer to the top and the bottom sides of the films.

### 3.2 XRD analysis of the blend films

The XRD patterns of both sides of the PVA/starch/Gly and PVA/starch/Gly-Sor films are shown in Figure 2. The peaks at  $2\theta \approx 11.6^\circ$  and  $\approx 19.6^\circ$  in all films can be attributed to the PVA crystals. The peak at  $2\theta \approx 20.2^\circ$  indicated that PVA had the pseudo-crystalline structure of an orthorhombic lattice.<sup>34</sup> Both sides of the PVA/NCS/Gly and PVA/NCS/Gly-Sor showed similar patterns. However, pronounced differences were observed between the diffraction patterns from the top and bottom sides of blend films based on the HCS and PCS. The plasticized PVA/HCS and PVA/PCS films, the patterns from the top side were dominated by the diffraction patterns of PVA, while the patterns from the bottom side showed the additional peaks at  $2\theta \approx 17.3^\circ$  and  $\approx 22.4^\circ$  which were attributed to the diffraction of V<sup>-26</sup> and A-type<sup>35</sup> starch derived from the amylose component.<sup>35,36</sup> These patterns pointed to the formation of a simple helical inclusion complex between amylose and glycerol by H-bonding as suggested previously.<sup>37</sup> It was reported that XRD patterns of PCS flake and PCS/Gly film showed no diffraction peak<sup>6</sup> due to pronounced amorphization during gelatinization process.<sup>38</sup> Surprisingly in this work, the PVA/PCS/Gly and PVA/PCS/Gly-Sor blend films showed the diffraction patterns of starch at the bottom side, suggesting the crystalline structure was restored in the blend. The formation of PVA-rich or starch-rich phases did not depend on the nature of the plasticizer.

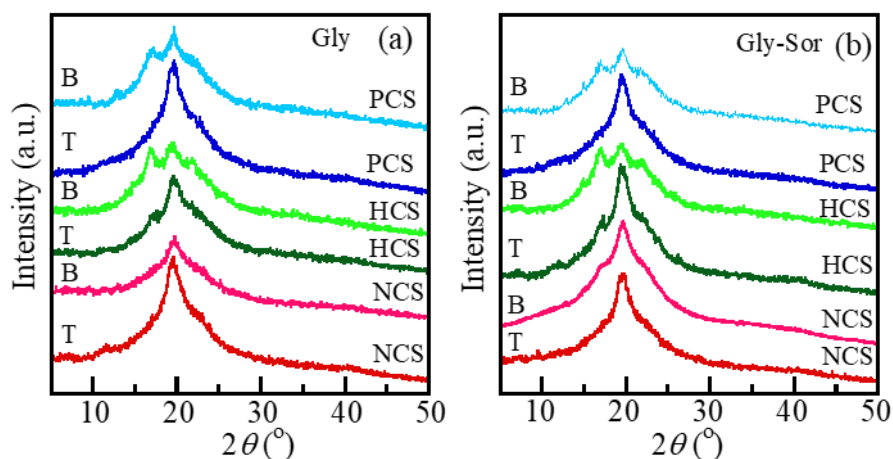


**Figure 2.** XRD patterns of (a) PVA/starch/Gly and (b) PVA/starch/Gly-Sor films. Types of starch are indicated. T and B refer to the top and the bottom sides of the films.

### 3.3 Differential scanning calorimetry

Melting temperature ( $T_m$ ), enthalpy of fusion ( $\Delta H_f$ ), and degree of crystallinity ( $X_c$ ) of the plasticized PVA/starch films were listed in Table 1. The neat PVA film showed  $T_g$  at 74.7°C and  $T_m$  at 174.9°C (Table S3 in the Supporting Information), whereas all plasticized blend films showed only  $T_m$  due to the plasticizing effect (Figure S2 in the Supporting Information). Moreover,  $T_m$  of the PVA/starch blend films shifted to higher temperature and  $X_c$  (except HCS-based films) compared to the plasticized PVA films indicating strong interaction between starch, PVA, and plasticizers as mentioned previously. The PVA/HCS/Gly blend films showed the lowest  $T_m$ ,  $\Delta H_f$  and  $X_c$  possibly due to the reduction of hydroxyl groups after oxidation process that could form hydrogen bonding with Gly molecules. On the other hand, the PVA/PCS/Gly films showed the highest  $T_m$  and  $X_c$ . This might be a result of the destruction of starch granules after pre-gelatinization<sup>19</sup> that improved miscibility between polymer blends and significantly enhanced chemical interactions between PCS and plasticizer.

**Table 1.** Melting temperature ( $T_m$ ), enthalpy of fusion ( $\Delta H_f$ ), and degree of crystallinity ( $X_c$ ) of the PVA/starch blend films.

Sample	2 <sup>nd</sup> heating scan		
	$T_m$ (°C)	$\Delta H_f$ (J g <sup>-1</sup> )	$X_c$ (%)
PVA/NCS/Gly	166.5	9.80	11.22
PVA/NCS/Gly-Sor	168.9	8.55	9.79
PVA/HCS/Gly	158.2	5.41	6.19
PVA/HCS/Gly-Sor	159.5	6.70	7.67
PVA/PCS/Gly	174.5	11.65	13.34
PVA/PCS/Gly-Sor	169.5	7.30	8.36

### 3.4 Mechanical properties

Tensile strength ( $TS$ ), elongation at break ( $EB$ ), Young's modulus ( $E$ ) of the neat PVA, PVA/starch/Gly and PVA/starch/Gly-Sor films are summarized in Table 2. The stress-strain plots of the blend films are shown in Figure 3. All the blend films had lower  $TS$  compared to that of neat PVA film due to the plasticizing effect and the addition of starch.<sup>26</sup> The plasticizer reduced the intermolecular forces and increased the polymeric chain mobility by increasing free space in the chains, generating the films with loosen matrix. When the films were subjected to the mechanical stress, the movement was facilitated by the plasticizer, and thus  $TS$  decreased.<sup>17</sup> With the same type of starch, the films containing Gly-Sor showed higher  $TS$  than Gly system due to the larger molecular structure of Sor ( $C_6H_{14}O_6$ ) than Gly ( $C_3H_8O_3$ ). Therefore, Gly had a greater ability to penetrate the PVA/starch matrix and showed stronger effect on an improvement of chain mobility.<sup>39</sup> These results agreed with the previous work that reported stronger and more rigid of the starch films plasticized with Sor than those with Gly. The large size of Sor limited the insertion into starch chains, thus the

effective in distribution was low.<sup>40</sup> Among three types of starch, PCS showed the highest *TS* confirming more interactions within the blend films. Note that, *TS* values of the PVA/NCS/Gly-Sor, PVA/HCS/Gly-Sor, PVA/PCS/Gly, and PVA/PCS/Gly-Sor films were superior to those reported for LDPE film (*TS*  $\approx$  10 MPa,<sup>41-45</sup> *TS*  $\approx$  13 MPa,<sup>46</sup> and *TS* = 6 MPa<sup>47</sup>).

**Table 2.** Tensile strength (*TS*), elongation at break (*EB*), and Young's modulus (*E*) of the neat PVA and PVA/starch blend films.

sample	<i>TS</i> (MPa)	<i>EB</i> (%)	<i>E</i> (MPa)
Neat PVA	44.20 $\pm$ 2.46	105 $\pm$ 13	86.21 $\pm$ 11.83
PVA/NCS/Gly	4.56 $\pm$ 0.42	178 $\pm$ 29	33.65 $\pm$ 11.24
PVA/NCS/Gly-Sor	9.25 $\pm$ 0.36	100 $\pm$ 11	269.83 $\pm$ 30.27
PVA/HCS/Gly	5.84 $\pm$ 0.40	348 $\pm$ 40	123.72 $\pm$ 20.10
PVA/HCS/Gly-Sor	10.81 $\pm$ 0.78	455 $\pm$ 19	197.69 $\pm$ 56.92
PVA/PCS/Gly	14.39 $\pm$ 0.76	504 $\pm$ 42	19.93 $\pm$ 2.57
PVA/PCS/Gly-Sor	15.81 $\pm$ 1.04	415 $\pm$ 22	300.97 $\pm$ 51.72

Compare with the neat PVA film, the addition of plasticizer increased *EB* of the films, except the PVA/NCS blend films, by increasing the molecular spaces in the matrix and reducing the hydrogen bonds between PVA chains<sup>17</sup> as mentioned in the previous section. According to the PVA/starch blends, using only Gly as the plasticizer yielded films with higher *EB* compared with the blends plasticized by Gly-Sor, except the PVA/NCS films. These results were consistent with *TS* values due to the better penetration of Gly molecules, and thus the more stretchability of the films. The PVA/PCS/Gly, PVA/HCS/Gly-Sor, and

PVA/PCS/Gly-Sor films showed very high values for  $EB$ , which exceeded that reported for LDPE film ( $\approx 400\%$ ).<sup>48</sup>

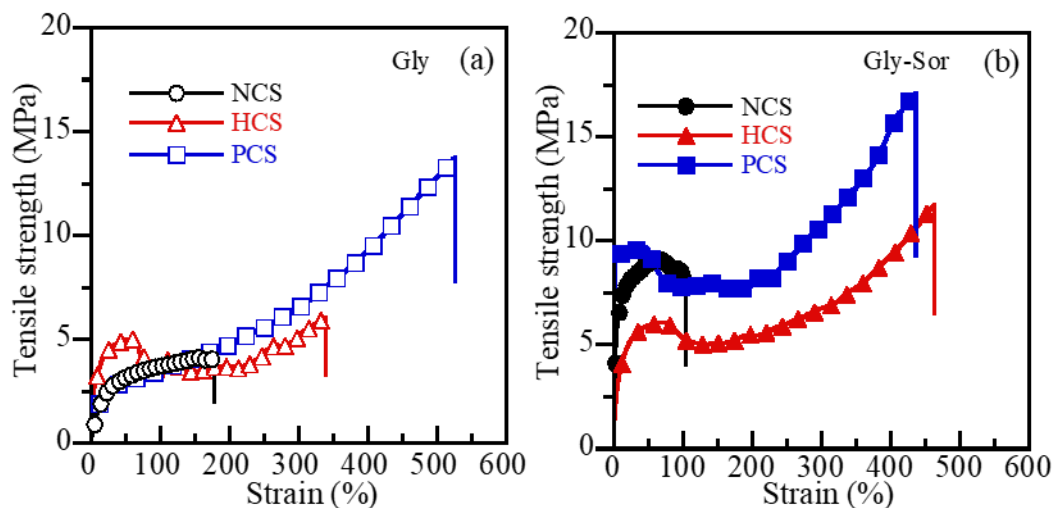


**Figure 3.** Stress-strain plots of (a) PVA/starch/Gly and (b) PVA/starch/Gly-Sor films.

Young's modulus ( $E$ ) represents the stiffness of the material.<sup>17</sup> From all types of starch, the Gly-Sor plasticized films showed higher  $E$  than the Gly plasticized films, indicating stronger and more rigid of the Gly-Sor plasticized films.<sup>49</sup> In addition, the effect of Gly-Sor over Gly was more pronounced for the PVA/NCS and PVA/PCS films. Among all films considered, it was clear that the PCS-based films with either Gly or Gly-Sor plasticizer were the best performing in terms of mechanical properties and would be ideal for applications that require a combination of strength with high levels of  $EB$ .

### 3.5 Morphology

Cryo-fractured cross-sections and samples after tensile testing of all the blend films were observed by SEM. The cryo-fractured cross-sections of all blend films showed rough surface layer and smooth surface layer (Figure 4(a-c, g-i)). These SEM micrographs confirmed the bilayer morphology. The surfaces of the samples after tensile testing showed

more damage on the surface of the starch-rich layer (marked with \* in the SEM micrographs) than the PVA-rich layer (Figure 4(d-f, j-l)). From the post-test surfaces, the starch-rich layer was more prone to tearing perpendicular to the direction of tension than the PVA-rich layer, that was less damaged and remained smooth. The presence of the PVA-rich layer led to the improvement in tensile properties of the blend films. However, for the case of the PVA/PCS/Gly film (Figure 4(f)), both sides of the film after tensile testing were smooth. This result was in agreement with the DSC results showing the highest  $X_c$ , suggesting that the adhesion at the interfaces between the starch-rich and PVA-rich phases was strong.

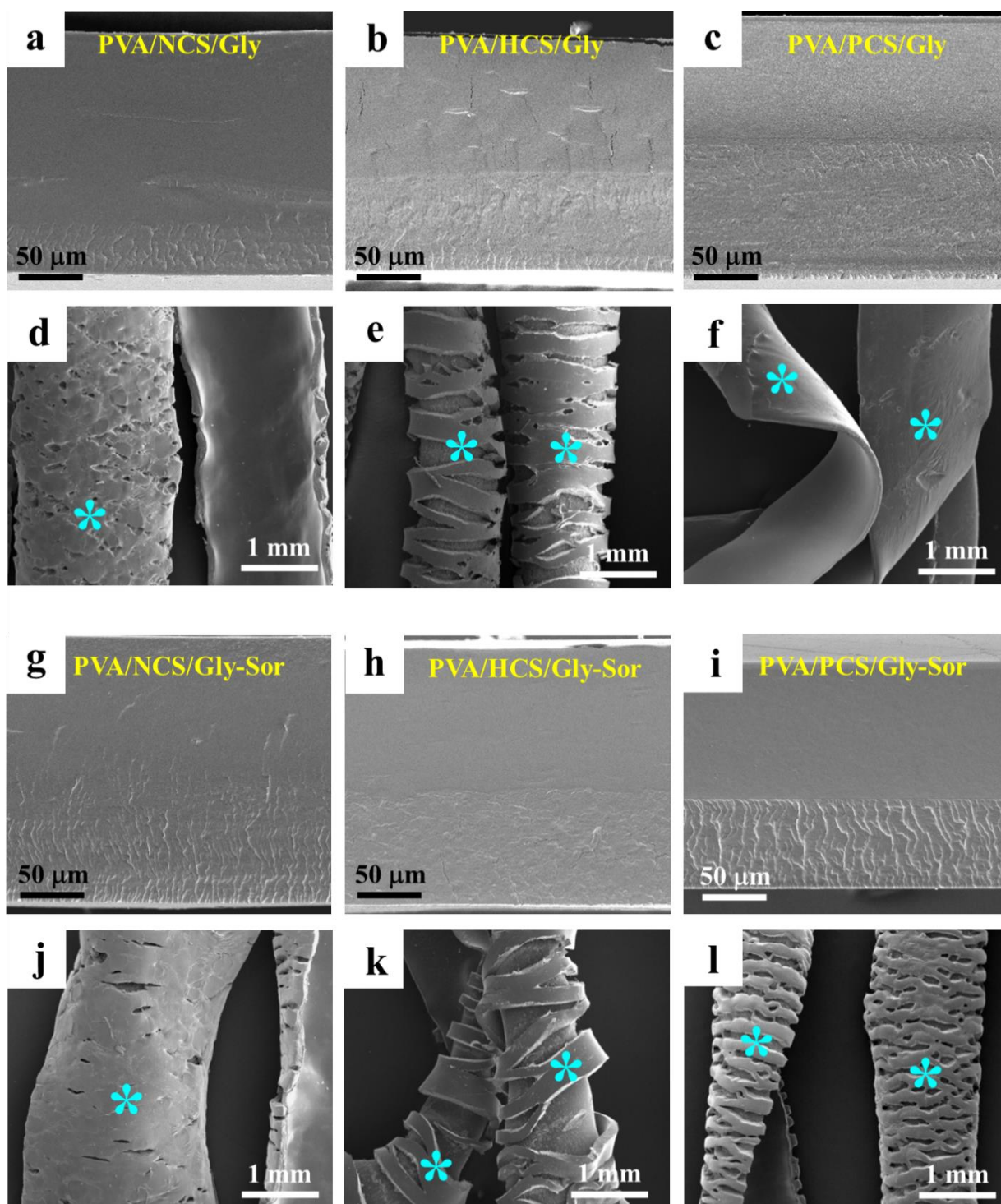


**Figure 4.** SEM micrographs are of (a-c, g-i) cryo-fractured cross-sections and (d-f, j-l) and the surfaces of PVA/starch blend films after tensile testing. Types of starch and plasticizer are indicated. The starch-rich layer marked with \*.



In enlarged SEM micrographs of tensile failure surfaces of the PVA/starch/Gly and PVA/starch/Gly-Sor films (Figure S3 in the Supporting Information), the rough surfaces at the bilayer interface of the PVA/HCS and PVA/PCS films, revealed some degree of adhesion between the starch-rich and PVA-rich phases, except in the PVA/PCS/Gly film (Figure S3(c)). It was clear in the SEM micrographs that Gly and Gly-Sor showed no influence on the bilayer morphology of the films, except on the PVA/PCS/Gly film after tensile testing (Figure 4(f)). The HCS- and PCS-based blend films formed a bilayer morphology irrespective of the presence of Gly or Gly-Sor.

### 3.6 Swelling test

All PVA/starch blend films after immersion in water were photographed. The swelling pictures of the PVA/starch/Gly and PVA/starch/Gly-Sor blend films are shown in Figure 5. The NCS-based films showed the highest DS (PVA/NCS/Gly =  $250 \pm 18\%$ , PVA/NCS/Gly-Sor =  $307 \pm 34\%$ ) (Figure 5(a, b)), as a result of the high population of free -OH groups. The DS of the blend films significantly decreased for HCS-based film (PVA/HCS/Gly =  $119 \pm 29\%$ , PVA/HCS/Gly-Sor =  $105 \pm 28\%$ ) (Figure 5(c, d)). It was reported that the addition of oxidized-cassava starch in native cassava starch reduced the swelling capacity of the film.<sup>15</sup> The reduction of swelling capacity of the film with the addition of the oxidized cassava starch was due to the internal crosslinks of dialdehyde through hemi-acetalization with hydroxyl groups of starch,<sup>50</sup> essentially enhancing the hydrophobicity of the film. Thus, the hydrophobicity of the film increased. The PVA/PCS films were in a gel-like condition after immersion in water for 24 h (Figure 5(e, f)). Even though the PCS based blends showed the crystalline structure of starch determined by the XRD analysis, the films broke into small pieces, precluding the calculation of DS.

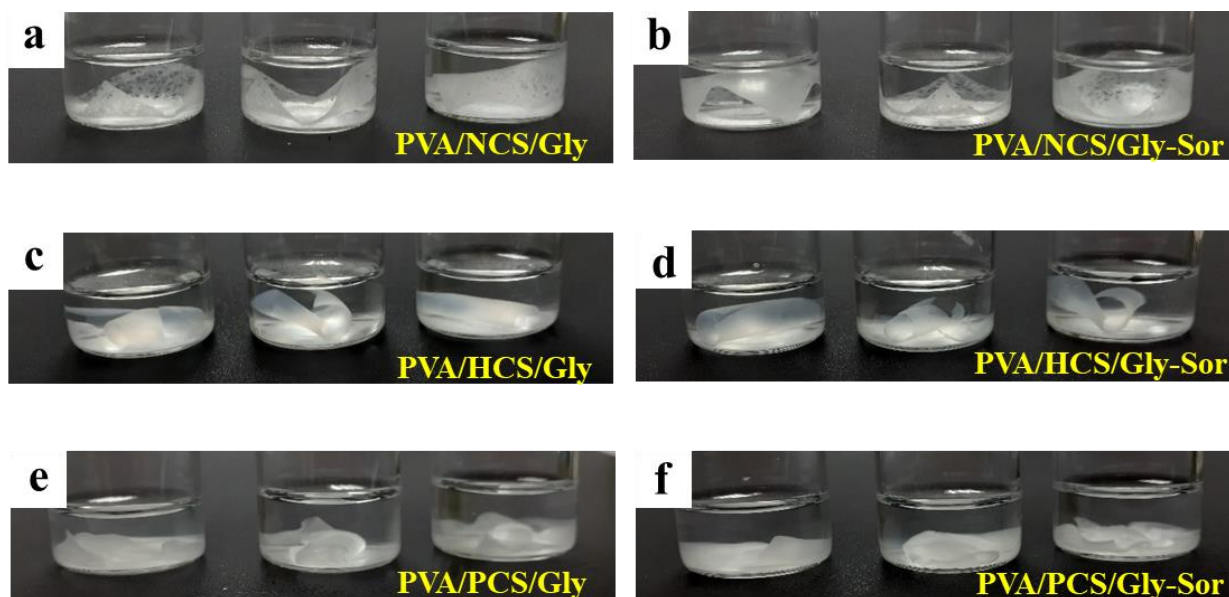


**Figure 5.** Photographs of PVA/starch blend films after 24 h in water at room temperature.

Types of starch and plasticizer are indicated.

### 3.7 Soil burial test

After burial in soil, all the PVA/NCS and PVA/PCS blend films were degraded within 1 day, suggesting the faster degradation of the PVA component. These results were consistent with the complete dissolution in water after 24 h of the PVA/Gly and PVA/Gly-Sor films. The PVA/HCS films exhibit the slowest degradation rate, an effect directly related to their lowest DS and remained partially intact after 3 days but were fully degraded within 4 days (Figure 6). The lowest biodegradation rate of the PVA/HCS films agreed with the least swelling degree of the films. The solubility of the film in water determined the biodegradability when the film was used as a packaging material.<sup>51</sup> Low solubility could indicate high water resistance.<sup>52</sup> Whereas, higher solubility of the films leads to higher biodegradability.<sup>53-54</sup> High or complete solubility of the films can be helpful for biodegradation, whereas its low solubility was suitable for storage.<sup>18</sup> Among the plasticized blend films, the plasticized PVA/PCS films showed the highest swelling capacity in water, therefore their rate of degradation was the highest due to the loss of crystalline structure of

starch. It was reported that the more biodegradation occurred due to the increasing water uptake of the PVA component.<sup>55</sup>

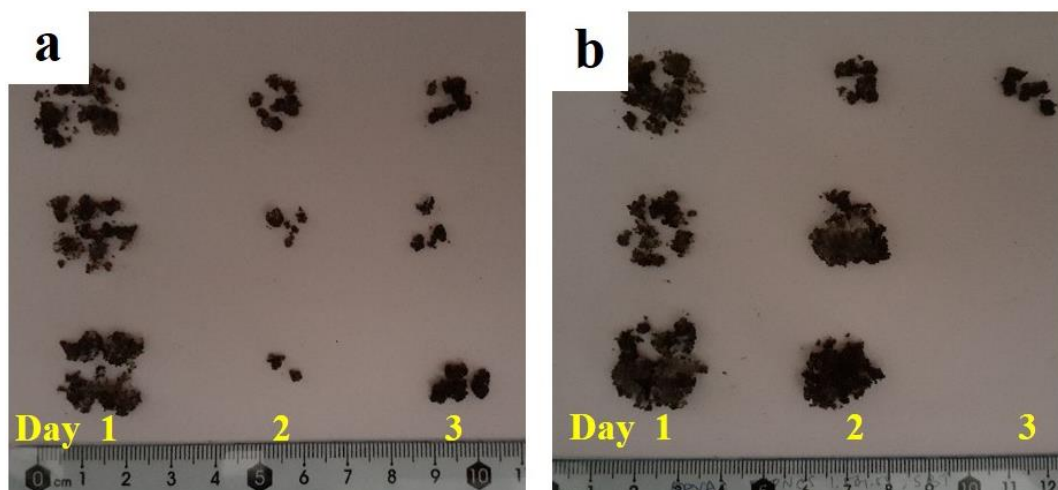


**Figure 6.** The photographs of the (a) PVA/HCS/Gly and (b) PVA/HCS/Gly-Sor blend films after buried in soil for 1, 2 and 3 days.

#### 4. Conclusions

The structure, morphology, mechanical properties and thermal behavior of a series of the PVA/starch blends plasticized by glycerol and glycerol-sorbitol mixture are reported in this study. In all films comprising modified cassava starch, a PVA-rich/starch-rich bilayer structure was observed, regardless the nature of the plasticizer. The addition of glycerol-sorbitol mixture increased tensile strength of the films. Incorporation of PVA to the blend films yielded high tensile strength and elongation at break but exhibited low degree of crystallinity. It was demonstrated here that the PCS-based blend films exhibited fast biodegradation kinetics, while showing superior mechanical properties as well as high degree of crystallinity among PVA/starch blend films. These results indicated that those novel blends have significant potential for a range of environmentally benign real-life applications.

**Acknowledgements**

This work is partly supported by the Faculty of Science Research Fund, Prince of Songkla University (contract number 158007).

## References

- [1] S. D. Yoon, *J. Agricultural Food Chem.* **2014**, *62*, 1755.
- [2] R. Jayasekara, I. Harding, I. Bowater, G. B. Y. Christie, G. T. Lonergan, *J. Polym. Environ.* **2003**, *11*, 49.
- [3] R. Jayasekara, I. Harding, I. Bowater, G. B. Y. Christie, G. T. Lonergan, *Polym. Test.* **2004**, *23*, 17.
- [4] P. Boonsuk, A. Sukolrat, S. Bourkaew, K. Kaewtatip, S. Chantarak, A. Kelarakis, C. Chaibundit, *Int. J. Biol. Macromol.* **2021**, *167*, 130.
- [5] J. Arayaphan, P. Boonsuk, S. Chantarak, *Iranian Polymer Journal* **2020**, *29*, 749.
- [6] P. Boonsuk, A. Sukolrat, K. Kaewtatip, S. Chantarak, A. Kelarakis, C. Chaibundit, *J. Appl. Polym. Sci.* **2020**, DOI: 10.1002/APP.48848
- [7] Y. Liu, K. Li, J. Pan, B. Liu, S. S. Feng, *Biomaterials* **2010**, *31*, 330.
- [8] R. L. Shogren, J. W. Lawton, K. F. Tiefenbacher, L. Chen, *J. Appl. Polym. Sci.* **1998**, *68*, 2129.
- [9] A. Corti, P. Cinelli, S. D'Antone, E. -R. Kenawy, R. Solaro, *Macromol. Chem. Phys.* **2002**, *203*, 1526.
- [10] C. C. DeMerlis, D. R. Schoneker, *Food Chem. Toxicol.* **2003**, *41*, 319.
- [11] R. L. Shogren, J. W. Lawton, K. F. Tiefenbacher, L. Chen, *J. Appl. Polym. Sci.* **1998**, *68*, 2129.
- [12] D. Kuakpetoon, Y. J. Wang, *Starch/Stärke* **2001**, *53*, 211.
- [13] K. Sangseethong, S. Lertphanich, K. Sriroth, *Starch/Stärke* **2009**, *61*, 92.
- [14] K. Sangseethong, N. Termvejsayanon, K. Sriroth, *Carbohydr. Polym.* **2010**, *82*, 446.
- [15] O. O. Oluwasina, F. K. Olaleye, S. J. Olusegun, O. O. Oluwasina, N. D. S. Mohallem, *Int. J. Biol. Macromol.* **2019**, *135*, 282.

- [16] A. Sarkar, D. R. Biswas, S. C. Datta, B. S. Dwivedi, R. Bhattacharyya, R. Kumar, K. K. Bandyopadhyay, M. Saha, G. Chawla, J. K. Saha, A. K. Patra, *Carbohydr. Polym.* **2021**, *259*, 117679.
- [17] L. M. Fonseca, A. K. Henkes, G. P. Bruni, L. A. N. Viana, C. M. de Moura<sup>1</sup>, W. H. Flores, A. F. Galio, *Food Biophys.* **2018**. <https://doi.org/10.1007/s11483-018-9522-y>
- [18] V. Hiremani, T. Gasti, S. Satareddi, V. N. Vanjeri, N. Goudar, S. Masti, R. Chougale, *Chemical Data Collections* **2020**, doi: <https://doi.org/10.1016/j.cdc.2020.100416>
- [19] S. C. Alcázar-Alay, M. A. A. Meireles, *Food Sci. Technol.* **2015**, *35*, 215-236.
- [20] C. W. Chiu, D. Solarek, In *Starch Chemistry and Technology 3<sup>rd</sup> Edition*; BeMiller, J.; Whistler, R., Eds.; Academic Press: New York, 2009, Chapter 17.
- [21] W. H. Teklehaimanot, S. S. Ray, M. N. Emmambu, *J. Cereal Sci.* **2020**, *95*, 103083. <https://doi.org/10.1016/j.jcs.2020.103083>
- [22] B. Siddaraamaiah Raj, R. Somashekar, *J. Appl. Polym. Sci.* **2004**, *91*, 630.
- [23] B. Ramaraj, *Polym. Plast. Technol. Eng.* **2006**, *45*, 1227.
- [24] Y. Chen, X. Cao, P. R. Chang, M. A. Huneault, *Carbohydr. Polym.* **2008**, *73*, 8.
- [25] X. Luo, J. Li, X. Lin, *Carbohydr. Polym.* **2012**, *90*, 1595.
- [26] P. A. Seekumar, M. A. Al-Harhi, S. K. De, *J. Appl. Polym. Sci.* **2012**, *123*, 135.
- [27] A. Cano, E. Fortunati, M. Cháfer, J. M. Kenny, A. Chiralt, C. González-Martínez, *Food Hydrocoll.* **2015**, *48*, 84.
- [28] H. R. Park, H. R. Chough, Y. H. Yun, S. D. Yoon, *J. Polym. Environ.* **2005**, *13*, 375.
- [29] R. A. Talja, H. Helén, Y. H. Roos, K. Jouppila, *Carbohydr. Polym.* **2008**, *71*, 269.
- [30] H. Tian, J. Yan, A. V. Rajulu, A. Xiang, X. Luo, *Int. J. Biol. Macromol.* **2017**, *96*, 518.
- [31] Y. Nishio, T. Haratani, T. Takahashi, R. S. J. Manley, *J. Macromolecules* **1989**, *22*, 2547.

- [32] L. Dai, J. Zhang, F. Cheng, *Int. J. Biol. Macromol.* **2019**, *132*, 897.
- [33] K. Kačuráková, M. Mathlouthi, *Carbohydr. Res.* **1996**, *284*, 145.
- [34] X. Han, S. Chen, X. Hu, *Desalination* **2009**, *240*, 21.
- [35] R. Kumar, A. Kumar, N. K. Sharma, N. Kaur, V. Chundri, M. Chawla, S. Sharma, K. Singh, M. Garg, *PloS One* **2016**, *11*, Article e0147622.
- [36] W. Li, Y. Shan, X. Xiao, Q. Luo, J. Zheng, S. Ouyang, G. Zhang, *J. Agric. Food Chem.* **2013**, *61*, 6477.
- [37] S. H. Imam, D. F. Wood, M. A. Abdelwahab, B. S. Chiou, T. G. Williams, G. M. Glenn, W. J. Orts, *Starch-Based Polymeric Materials and Nanocomposites: Chemistry, Processing, and Applications* (Eds: Ahmed, J., Tiwari, B., Imam, S., and Rao, M.), CRC Press Taylor & Francis Group, USA 2012, pp. 5–32.
- [38] M. Majzoobi, M. Radi, A. Farahnaky, J. Jamalian, T. Tongdang, G. J. Mesbahi, *G. J. Agric. Sci. Tech.* **2011**, *13*, 193.
- [39] A. B. Dias, C. M. O. Müller, F. D. S. Larotonda, J. B. Laurindo, *J. Cereal Sci.* **2010**, *51*, 213.
- [40] T. Wittaya, *Curr. Appl. Sci. Technol.* **2013**, *13*, 51.
- [41] W. T. Mead, R. S. Porter, *Applied Polymer* **1978**, *22*, 3249.
- [42] P. K. Sastry, D. Satyanarayana, D. V. M. Rao, *J. Appl. Polym. Sci.* **1998**, *70*, 2251.
- [43] R. Satoto, M. Karina<sup>1</sup>, A. H. D. Abdullah, P. Nugroho, *J. Mater. Environ. Sci.* **2019**, *10*, 706.
- [44] C. Y. Chee, N. L. Song, L. C. Abdullah, T. S. Y. Choong, A. Ibrahim, T. R. Chantara,

*Journal of Nanomaterials* Volume 2012, Article ID 215978, 6 pages.

doi:10.1155/2012/215978.

[45] R. Strapasson, S. C. Amico, M. F. R. Pereira, T. H. D. Sydenstricker, *Polym. Test.* **2005**, *24*, 468.

[46] T. J. Herald, E. Obuz, W. W. Twombly, K. D. Rausch, *Cereal Chem.* **2002**, *79*, 261.

[47] S. Arunwisut, S. Phummanee, A. Somwangthanoj, *J. Appl. Polym. Sci.* **2007**, *106*, 2210.

[48] P. K. Sastry, D. Satyanarayana, D. V. M. Rao, *J. Appl. Polym. Sci.* **1998**, *70*, 2251.

[49] S. Mali, L. S., Sakanaka, F. Yamashita, M. V. E. Grossmann, *Carbohydr. Polym.* **2005**, *60*, 283.

[50] U. Shah, F. Naqash, A. Gani, F. A. Masoodi, *Compr. Rev. Food Sci. Food Saf.* **2016**, *15*, 568.

[51] T. Bourtoom T, S. M. Chinnan, *LWT - Food Sci. Technol.* **2008**, <https://doi.org/10.1016/j.lwt.2007.10.014>.

[52] V. D. Hiremani, S. Sataraddi, P. K. Bayannavar, T. Gasti, S. P. Masti, R. R. Kamble, R. B. Chougale, *SN Appl. Sci.* **2020**, *2*, 1877.

[53] L. Nouri, A. Mohammadi Nafchi, *Int. J. Biol. Macromol.* **2014**, *66*, 254.

[54] R. B. De Pauli, L. B. Quast, I. M. Demiate, L. S. Sakanaka, *Starch/Stärke* **2011**, *63*, 595.

[55] R. Lim, P. L. Kiew, M. K. Lam, W. M. Yeoh, M. Y. Ho, *Asia-Pac. J. Chem. Eng.* **2021**; e2622. <http://doi.org/10.1002/apj.2622>.